Elsevier Editorial System(tm) for BBA - Biomembranes
Manuscript Draft

Manuscript Number:

Title: Two homologous neutrophil serine proteases bind to POPC vesicles with different affinities: when aromatic amino acids matter

Article Type: Regular Paper

Keywords: amphitropic protein;
large unilamellar vesicles;
molecular dynamics simulations;
surface plasmon resonance;
proteinase 3;
neutrophil elastase

Corresponding Author: Dr. Nathalie Reuter, PhD

Corresponding Author's Institution:

First Author: Anne-Sophie Schillinger

Order of Authors: Anne-Sophie Schillinger; Cedric Grauffel, PhD; Øyvind Halskau, PhD; Nathalie Reuter, PhD

Abstract: Neutrophil serine proteases Proteinase 3 (PR3) and human neutrophil elastase (HNE) are homologous antibiotic serine proteases of the polymorphonuclear neutrophils. Despite sharing a 56% sequence identity they have been shown to have different functions and localizations in the neutrophils. In particular, and in contrast to HNE, PR3 has been detected at the outer leaflet of the plasma membrane and its membrane expression is a risk factor in a number of chronic inflammatory diseases. Although a plethora of studies performed in various cell-based assays have been reported, the mechanism by which PR3, and possibly HNE bind to simple membrane models remains unclear. We used Surface Plasmon Resonance (SPR) experiments to measure and compare the affinity of PR3 and HNE for large unilamellar vesicles composed of 1-palmitoyl-2-oleoyl-sn-glycero-3-phosphocholine (POPC). We also conducted 500-ns long molecular dynamics simulations of each enzyme at the surface of a POPC bilayer to map the interactions between proteins and lipids and rationalize the difference in affinity observed in the SPR experiment. We find that PR3 binds strongly to POPC large unilamellar vesicles (Kd = 9.2x10-7 M) thanks to the insertion of three phenylalanines, one tryptophane and one leucine beyond the phosphate groups of the POPC lipids. HNE binds in a significantly weaker manner (Kd > 33.4x10-7 M) making mostly electrostatic interactions via lysines and arginines and inserting only one leucine between the hydrophobic lipid tails. Our results support the early reports that PR3, unlike HNE, is able to directly and strongly anchor directly to the neutrophil membrane.

Suggested Reviewers: Emma Sparr
Professor, Department of Chemistry, University of Lund
emma.Sparr@fkem1.lu.se
Expertise in protein-lipid interaction and physical chemistry methods to study the above-mentioned

Gregor Anderluh
Professor, Laboratory for Molecular Biology and Nanobiotech, National Institute of Chemistry

gregor.anderluh@ki.si
Expertise in the use of Surface Plasmon Resonance for studies of protein-lipid interactions, and in particular interactions of proteins with lipid vesicles

Luca Monticelli
Senior Researcher, Institut de Biologie et Chimie des Protéines, CNRS
luca.monticelli@inserm.fr
Expertise in molecular simulations of membrane models (incl. lipid bilayers), and protein-lipid interactions

Robert Stahelin
Adjunct Associate Professor, Department of Chemistry & Biochemistry, University of Notre Dame
rstaheli@nd.edu
Expertise in physico-chemical studies of membrane recruitment of peripheral proteins, including Surface Plasmon Resonance

Jeffery Klauda
Assistant Professor, A. James Clark School of Engineering, University of Maryland
jbklauda@umd.edu
Expertise in molecular dynamics simulations of peripheral membrane binding proteins, development of the lipids update for the CHARMM force field

UNIVERSITY OF BERGEN
Department of Molecular Biology
Computational Biology Unit

Nathalie Reuter, PhD

BBA - Biomembranes
Editor-in-Chief

Bergen, 11 February 2014

Dear Madam, Sir,

Please find enclosed a manuscript entitled " ***Two homologous neutrophil serine proteases bind to POPC vesicles with different affinities: when aromatic amino acids matter***", by Anne-Sophie Schillinger, Cédric Grauffel, Øyvind Halskau and Nathalie Reuter, that we wish to submit for publication as a Regular Paper in BBA Biomembranes.

Proteinase 3 and the Human Neutrophil Elastase are two antibiotic serine proteases of the polymorphonuclear neutrophils.

Beyond their importance as therapeutic targets, their sequence and structural similarity makes them a relevant model for comparative study of membrane insertion. …

Using a combination of molecular dynamics simulations and surface plasmon resonance experiments, we show that PR3 binds to large unilamellar vesicles with a higher affinity and HNE. The SPR sensorgrams clearly indicate …. different k_{off} Nest 500 ns-long molecular dynamics simulations of each protein reveal a striking difference between the proteins interfacial binding sites: PR3 has xxx aromatic amino acids inserted in-between the lipid tails while HNE has only YYYY.

Our manuscript reports thus two important findings. The first one being that Proteinase 3 binds strongly to membrane models, indicating that it might bind directly to cell membranes. This is of relevance for …. The second finding is of broader relevance for the field of protein-lipid interactions and is the impact of the insertion of aromatic amino acids for peripheral membrane binding

We believe that this work is of interest for the readership of BBA Biomembranes and we hope that you will consider it favorably.

We thank you in advance for your handling of this manuscript.
Yours sincerely,

On behalf of all the authors,

Nathalie REUTER, PhD

Two homologous neutrophil serine proteases bind to POPC vesicles with different affinities: when aromatic amino acids matter

Anne-Sophie SCHILLINGER[1,2], Cédric GRAUFFEL[1,2], Øyvind HALSKAU[1], Nathalie REUTER[1,2*]

[1] Department of Molecular Biology, University of Bergen, Pb. 7803, N-5020 Bergen, Norway

[2] Computational Biology Unit, Department of Informatics, University of Bergen, Pb. 7803, N-5020 Bergen, Norway

A.-S.S.: Anne-Sophie.Schillinger@mbi.uib.no

O.H.: Oyvind.Halskau@mbi.uib.no

C.G.: cedric@ibms.sinica.edu.tw

* To whom correspondence should be addressed:

Nathalie Reuter, University of Bergen, Department of Molecular Biology, Pb. 7803, N-5020 Bergen, Norway

Tel: (+47) 555 84040 // Fax: (+47) 555 89683

E-mail address: nathalie.reuter@mbi.uib.no

Present address:

For Cédric Grauffel: Institute of Biomedical Sciences, Academia Sinica, Taipei 115, Taiwan

ABSTRACT

Neutrophil serine proteases Proteinase 3 (PR3) and human neutrophil elastase (HNE) are homologous antibiotic serine proteases of the polymorphonuclear neutrophils. Despite sharing a 56% sequence identity they have been shown to have different functions and localizations in the neutrophils. In particular, and in contrast to HNE, PR3 has been detected at the outer leaflet of the plasma membrane and its membrane expression is a risk factor in a number of chronic inflammatory diseases. Although a plethora of studies performed in various cell-based assays have been reported, the mechanism by which PR3, and possibly HNE bind to simple membrane models remains unclear. We used Surface Plasmon Resonance (SPR) experiments to measure and compare the affinity of PR3 and HNE for large unilamellar vesicles composed of 1-palmitoyl-2-oleoyl-sn-glycero-3-phosphocholine (POPC). We also conducted 500-ns long molecular dynamics simulations of each enzyme at the surface of a POPC bilayer to map the interactions between proteins and lipids and rationalize the difference in affinity observed in the SPR experiment. We find that PR3 binds strongly to POPC large unilamellar vesicles (K_d = 9.2 x 10^{-7} M) thanks to the insertion of three phenylalanines, one tryptophane and one leucine beyond the phosphate groups of the POPC lipids. HNE binds in a significantly weaker manner (K_d > 33.4 x 10^{-7} M) making mostly electrostatic interactions via lysines and arginines and inserting only one leucine between the hydrophobic lipid tails. Our results support the early reports that PR3, unlike HNE, is able to directly and strongly anchor directly to the neutrophil membrane.

KEYWORDS: amphitropic protein, large unilamellar vesicles, molecular dynamics simulations, SPR: surface plasmon resonance, proteinase 3, neutrophil elastase

ABBREVIATIONS

PR3: proteinase 3, HNE: human neutrophil elastase, LUV: large unilamellar vesicle, POPC: 1-palmitoyl-2-oleoyl-sn-glycero-3-phosphocholine, SPR: surface plasmon resonance, MD: molecular dynamics

1. Introduction

Neutrophils are the most abundant type of leukocytes and are key components of the innate immune system, able to mediate both anti-infectious and pro-inflammatory effects [1, 2]. Neutrophil serine proteases (NSPs) Proteinase 3 (PR3, EC 3.4.21.76) and human neutrophil elastase (HNE) are homologous antibiotic serine proteases of the polymorphonuclear neutrophils (PMNs) which are therapeutic targets in a number of chronic inflammatory diseases[3]. PR3 and HNE are mainly localized in the azurophilic granules of resting neutrophils and externalized when the neutrophils are activated. Despite sharing a 56% sequence identity (Figure 1) and a high structural similarity (Cf. Figure 2A)[4] PR3 and HNE have been shown to have different functions and localizations in the neutrophils. In particular, and in contrast to HNE, PR3 has been detected at the surface of secretory vesicles and on the outer leaflet of the plasma membrane[5, 6]. The membrane expression of PR3 has been suggested as a pathogenic factor in chronic inflammatory diseases involving neutrophils [6-10].

Witko-Sarsat et al. first reported a specific association of PR3 to the plasma membrane, which they described as stronger "*than only an ionic interaction"*[11]. On the other hand Campbell et al. argued in favor of a weak charge-dependent mechanism similar for both proteases[12]. In agreement with the work of Witko-Sarsat et al., Goldman et al. showed using spectrophotometry techniques that PR3 and HNE bind with different affinities to reconstituted lipid bilayers[13]. Using bilayers with different ratios of zwitterionic (DMPC[1]) and anionic (DMPG[2]) phospholipids, they showed that while PR3 binds to DMPC vesicles with an estimated K_d of 85 μM.

[1] DMPC:dimyristoylphosphatidylcholine
[2] DMPG:dimirystoylphosphatdylglycerol

HNE wasn't observed to bind to pure DMPC vesicles but binds to mixed DMPC:DMPG 1:1 liposomes with a K_d of 14.5 μM. The authors also show that PR3 binds best to DMPC:DMPG 1:1 vesicles with a K_d of 4.5 μM. Moreover results from differential scanning calorimetry and hydrophobic photolabelling indicate that PR3 inserts amino acids into the hydrophobic region of the lipid vesicles, while HNE does it to a lesser extent. In 2004, Durant et al. used PR3 and HNE cDNA transfected mast cell lines and showed that PR3 was expressed at the cell surface after induced degranulation while HNE was released into the extra-cellular medium. Using molecular dynamics simulations with at first a simple membrane model [14], we have reported that PR3 inserts aromatic and aliphatic amino acids into the hydrophobic core of the bilayer models, while HNE interacts mostly via electrostatic interactions to the bilayer interface. We further used relatively short MD simulations (50 ns) of PR3 with explicit DMPC bilayers to describe the protein-lipid interactions at the atomic level of detail [15]. We reported an interface-binding site (IBS) composed of a few basic amino acids (R177, R186A[3], R186B, K187, R222) that ensure proper orientation of PR3 towards the membrane to allow for the insertion of a hydrophobic patch (V163, F165, F166, I217, W218, L223, F224) (Figure 2B). Mutations of four hydrophobic (F165, F166, L223, F224) or four basic amino acids (R186A, R186B, K187, R222) significantly affects the membrane expression of PR3 in a cell-based assay, thus validating the role of the predicted IBS for PR3 membrane expression [16]. Taken altogether these studies indicate that despite their high sequence similarity, PR3 and HNE interact with lipid membranes using different types of interactions. This is further supported by the amino acid substitutions in the region of

[3] We use the chymotrypsin numbering for both PR3 and HNE. It presents the advantage of providing a consistent numbering for all enzymes of the family but introduces letters in addition to the numbering (e.g the two consecutive arginines labelled 186A and 186B).

the PR3 IBS (Cf Figure 2) where in particular two of the three phenylalanines, as well as tryptophane W218, are substituted by non-aromatic residues in HNE.

A number of proteins have been shown to be co-localized and some, co-immunoprecipitated, with membrane-expressed PR3 and have been proposed as partners of PR3 at the neutrophil membrane (reviewed in refs [9, 17]): CD177 (NB1) [17, 18], Fcgamma receptor FcγRIIIb and $p22^{phox}$ subunit of cytochrome b558 [19], β2 integrin adhesion molecule CD11b/CD18[20], Protease Activated Receptor 2 (PAR2) [21, 22] and Phospholipid Scramblase 1 [23]. Interestingly fluorescence spectroscopy and confocal microscopy on CHO cells expressing NB1 revealed the presence of PR3 at the cell surface while this was not the case for cells that were not expressing NB1. This lead Korkmaz and co-workers to propose CD177 as a membrane receptor to which PR3 would bind through F166, I217, W218, L223 and F224 [24]. This corresponds closely to the region that we had earlier suggested as direct anchor of PR3 into the membrane hydrophobic region.

Yet, to our knowledge, there exist little evidence of a physical interaction between membrane-bound PR3 and the identified partners. Direct interaction of PR3 with the membrane phospholipids and interaction with protein partners are not mutually exclusive if we consider the formation of a protein complex. Interactions of membrane-bound PR3 with proteins, possibly transmembrane receptors, are indeed necessary for the function of PR3 and would stabilize its interactions with the membrane. Thus, in this work we do not discount the possible importance of protein-protein interactions, but focus on investigating the molecular details of PR3 and HNE anchoring to the lipid membrane. The available data to date has been obtained by different teams using a wide range of approaches and models, from cell-based assays

to molecular modeling, but only one study using standard biophysics methods in 1999[13].

Surface Plasmon Resonance has been successfully used to study interactions between lipid vesicles and proteins and can be used to obtain accurate values of dissociation constants (K_d)[25, 26]. Molecular dynamics simulations using all-atoms lipid bilayers provide a detailed map of the lipid-protein interactions, and for example the respective contributions of hydrophobic and polar amino acids (see for example Refs.[27-29]). Both methods are thus complementary as they provide information at different levels of resolution.

We here report a combined *in vitro* and *in silico* study investigating the affinity of PR3 and HNE for model membranes constituted of POPC lipids, more physiologically relevant than DMPC. We use SPR to characterize the affinity of PR3 and HNE for large unilamellar vesicles (LUVs) and 500-nanoseconds long molecular dynamics simulations of the two enzymes at the surface of a pre-equilibrated POPC bilayer to map the interactions between proteins and lipids at the atomic level of detail. The use of SPR allows us to obtain insights, albeit limited, into the kinetics of PR3 and HNE binding to POPC vesicles.

2. Material and Methods

2.1 Molecular dynamics simulations

We performed MD simulations of PR3 and HNE inserted in POPC lipid bilayers using the following procedure: (1) equilibration of the lipid bilayer, (2) insertion of PR3 in the lipid bilayer and (3) simulation of the PR3-POPC complex and subsequent analysis of the resulting trajectories.

In this manuscript we consequently use the chymotrypsin numbering for both PR3 and HNE. It presents the advantage of providing a consistent numbering for all enzymes of the family but introduces letters in addition to the numbering (e.g the two consecutive arginines labelled 186A and 186B).

POPC bilayer. A lipid bilayer made of 256 POPC was built using the CHARMM-GUI[30]. The lipid bilayer was subjected to energy minimization using NAMD[31] and the CHARMM36 force field update for lipids[32]. The system was then equilibrated without surface tension for 300 ps at 310 K using a time step of 2 fs and velocities reassignment every 500 fs, and subsequently run into production for 80 ns. The SHAKE algorithm was applied to constrain bonds between hydrogen and heavy atoms [33]. Non-bonded interactions were truncated using a cutoff of 12 Å, using a switch function for van der Waals and a shift function for electrostatics. For estimating long-range electrostatic forces, the Particle-Mesh-Ewald (PME) algorithm was used [34, 35]. The Langevin algorithm was used to control temperature (310K, damping coefficient: 1.0) and pressure (target pressure: 1 atm, oscillation period: 75 fs, oscillation decay time: 25 fs)[36]. The area per lipid and the order parameter were monitored along the simulation to assess the properties of the bilayer. The order parameter S_{CD} was calculated with VMD[37] from the mean value of the angle between each C-H bond of the lipid tails and the normal to the membrane. The profiles are consistent with those in Ref.[32]. The surface area was calculated to be 65.5 ± 0.8 Å on average during the simulation, close to that reported by Klauda et al. [32] (64.7 ± 0.2 Å) for a POPC bilayer simulated using the same CHARMM 36 force field. Kucerka et al. report an estimate of 68.3 ± 1.5 Å using hybrid electron density models[38].

Insertion of Proteinase 3 and HNE at the interface of the lipid bilayer. The cartesian coordinates of PR3 were taken from chain A of the X-ray structure referenced 1FUJ [39] in the RSCB Protein Data Bank,[40] and those of HNE from the 1PPF structure[41]. PR3 and HNE were then oriented with respect to, and inserted at, the interface of the equilibrated POPC lipid bilayer as described previously for PR3[15]. Briefly, each of the enzymes was positioned at the surface of a POPC lipid bilayer in the orientation predicted by implicit bilayer simulations for HNE [14] and using earlier all-atoms simulations with a DMPC bilayer for PR3[15]. PR3 was then translated 2 Å above its initial position to account for the difference in width between POPC and DMPC bilayers. Six lipids overlapping with the proteins were removed, in both the case of PR3 and HNE.

Simulations PR3-POPC and HNE-POPC. The systems were then minimized with CHARMM (v33b1)[42] using the following harmonic restraints: 150 kcal/mol/Å^2 on the protein backbone, water and ion molecules, 100 kcal/mol/Å^2 for membrane located further than 5 Å and 75 kcal/mol/Å^2 less than 5 Å from the protein and 10 kcal/mol/Å^2 for protein side chains located 5 Å or less from the membrane. The minimization consisted of 20 cycles of 500 steps of steepest descent and 100 steps of conjugate gradient algorithms with restraints being scaled by 0.65 after each cycle. The systems were then solvated in a cubic box of TIP3 water molecules [43] using VMD (version 1.8.7)[37]. A number of two and eleven chloride ions were added by replacing random water molecules to neutralize the system for PR3 and HNE, respectively. The system was subsequently equilibrated using NAMD[31] and Charmm force field (c27 with CMAP corrections) with two short runs of 400 ps in NVT ensemble, with velocities reassigned every 50 fs and 500 fs, and then further equilibrated for 2 ns. The integration of the equations of motion was done using a

Multiple Time Step algorithm [44]; bonded interactions and short-range nonbonded forces were evaluated in every step and long range electrostatics every second step. The system was then run into production for 500 ns in the NPT ensemble. Pressure and temperature control, as well as the cutoff scheme and treatment of long-range electrostatics interactions are the same as for the equilibration of the bilayer.

Analysis. Based on the evolution of the root mean square deviation (RMSD) between the trajectory conformations and the conformation of the enzymes before the MD simulations (Cf. supplementary data, Fig.S1), we decided to use the trajectories between 200 and 500 ns as sampling windows. All analyses described in the results section are thus performed on the last 300 nanoseconds of the simulations.

The occupancies of hydrogen bonds were calculated with the Charmm program [42] using a 2.4 Å cutoff distance between hydrogen and acceptor and a 130° donor-hydrogen-acceptor angle criterion. The donor and acceptor definition are taken from the Charmm force field (MacKerell, et al., 1998). Hydrophobic contacts were defined using a 3 Å cutoff distance between aliphatic group of the lipids and of the enzymes (Charmm atom types ca; cb; cg1; cg2; cg2; ha*; hb*; hg; hg2*; type cg except for hsd, hse, asn, asp; type hg1 except for cys, thr, ser; type cd except for arg, gln, glu; type cd1; type cd2 except for hsd, hse; type ce1, ce2, cz and associated hydrogens of phe, tyr, type cd1, cd2, ce2, ce3, cz2, cz3 and associated hydrogen of trp, type cay and type hy*). Cation-π interactions between aromatic rings (phenylalanine, tyrosine and tryptophan) are considered to exist when all distances between the heavy atoms of the aromatic ring and choline nitrogen are below 7 Å and when these distances do not differ by more than 1.5 Å (Chipot & Minoux, 1999; Petersen, Jensen, & Nielsen, 2005).

We evaluated the depth of anchorage of the proteins as described in Grauffel et al.[45]. Briefly we used the mean z coordinate of the phosphorus atoms as a reference plane. The center of mass of each residue was calculated and its difference to the reference plane was calculated. The *corman* module of the Charmm program was used for coordinates statistics. Values reported are means of the distances of the last 300 ns of simulations.

2.2 Sample preparation.

Proteins. PR3 and HNE were purchased from Athens Research & Technology and fatty acid free bovine serum albumine (BSA) from Sigma.

Liposomes. The lipids (POPC) were purchased from Avanti Polar Lipids. Liposomes were prepared as reported in (Jr, Ying, Baumann, & Kleppe, 2009). Lipids solvated in chloroform were added in glass tubes in the prerequisite amount. Lipids were handled and kept out of light and reactive atmosphere as much as possible by operation in hoods, flushing reagent bottles with dry N_2, and using glass containers wrapped in aluminum foil. The chloroform solutions were dried under dry N_2 pressure. Traces of chloroform were removed by subjecting the samples to vacuum for at least two hours. Lipid cakes were rehydrated with HBS-N buffer and vortexed vigorously until all films were suspended as slurry. For liposome-preparation, solutions were subjected to seven freeze-thaw cycles using liquid N_2 and a water bath. The hydrated multilamellar structures were then extruded at room temperature and well above the lipid T_m using a Mini-Extruder (Avanti Polar Lipids) assembled using two Millipore filters of 100 nm pore size. Samples were forced through the filters 10 times using Hamilton syringes and the resulting solutions were transferred to clean,

foil wrapped glass tubes and stored at 4°C. Final liposome composition was 100 % POPC and the total lipid concentration was 2.5 mM.

2.3 Surface Plasmon Resonance

The SPR analyses were carried out on a BIAcore T200 (BIAcore, GE Healthcare) and Biacore T200 Control Software. All experiments were carried at 25 °C. Protein and lipid interactions were monitored using a L1 sensor chip. A preparation procedure was performed before each experiment. The surface of the L1 sensor chip was first cleaned with a 1 min injection of 40 mM octylglucosyl at a flow rate of 10 µL/min. Liposome solutions were diluted to 1 mM concentration with running buffer (HBS-N: 0.1 M HEPES, 1.5 M NaCl, pH 7.4) and injected at a flow rate of 1 µL/min for 10 minutes until the maximum of binding was reached. Liposomes maximum deposition was about 8500 response units (RU) for POPC. The surface of the L1 chip was then washed with a solution of 10 mM NaOH for 1 min at a flow rate of 10 µL/min. The completeness of the chip coverage was assessed by injection of bovine serum albumin (BSA) at 0.1 mg/ml and at a rate of 10 µL/min for 60 s. Generally this injection did not perturb the lipid-covered chip by more than 43 RU, and it rapidly fell back to its original value when injection of BSA stopped. Binding assays were then performed on the validated chips. The two proteins (PR3 and HNE) were diluted to sets of at least 5 different concentrations ranging from 0.125 µM to 3 µM (0.125, 0.5, 1, 2, 3) and were injected over the immobilized liposomes at a flow rate of 5 µL/min for 120 s and 180 s (for HNE and PR3 respectively) until equilibrium was reached. The dissociation phase was measured for at least 420 s after the addition of the sample. At the end of the binding assay, the surface of the sensor chip was regenerated with a solution of octylglucosyl 40 mM for

30 s at a flow rate of 30 μL/min. No reference channel was used due to non-specific binding of PR3 on the chip [46]. Instead we focused on achieving maximal coverage of the chip with liposomes and in this way ensure that the resulting SPR signal was completely dominated by the protein interacting with the lipid membrane[47]. The SPR data were analysed with the Biacore T200 Evaluation Software. Binding affinities were calculated using the steady state affinity model (Langmuir model) and maximal resonance unit (RU) was plotted against concentration.

3. RESULTS

3.1 Molecular dynamics simulations

PR3 and HNE were positioned at the interfacial region of POPC lipid bilayers as described in the Methods section and illustrated on Figure 3A. Each system was simulated for 500 ns and analysed in order to characterize the interactions between the enzymes interfacial binding sites and the lipids. We report in Tables 1 and 2 the occupancy of significant hydrogen bonds along the sampling window (occupancy above 20%), as well as the average number of hydrophobic contacts for the amino acids that achieve on average more than one contact per frame of the trajectory. On Figure 3 we show a snapshot of the simulations of PR3 (Fig.3B) and HNE (Fig.3C).

3.1.1. PR3

The simulation indicates that the structure of PR3 is not affected by the presence of the membrane; the average RMSD between the conformations in the trajectory is 1.54±0.19 Å on the sampling window (Cf Fig.S1, Supplementary Data). PR3 remains at a stable depth of anchorage at the bilayer interface; we calculate a distance of

19.7±1.6 Å between the centre of mass of PR3 and the average plane of the phosphorus atoms (Cf. Supplementary Data, Fig.S2). Interactions between PR3 and the POPC bilayer are mediated almost exclusively by amino acids located on three different loops: β8-β9 (amino acids 163 to 180), β9-β10 (184-197), β11-β12 (215-225). The positions of PR3 amino acids with respect to the average plane of the phosphorus atoms gives an indication of their depth of anchorage in the lipid bilayer. Two loops are anchored significantly beyond the phosphorus atoms; loop β11-β12 appears to be the one that has the deepest anchorage. The β8-β9 loop with F165 and F166 is also anchored beyond the plane of the phosphorus atoms. The β9-β10 loop carries most of the basic cluster identified in our early implicit membrane simulations[14] and is positioned slightly above the two other ones.

Most of the hydrogen bonds we observe involve the phosphate groups of POPC lipids. A low number of hydrogen bonds with occupancies below 20% involve glycerol groups, only Arg186B[4] (58.7 %) and Arg222 (49.0 %) have occupancies of hydrogen bonds with glycerol above 20% indicating that they are buried somewhat deeper in the interface than the other basic amino acids. The strongest hydrogen bonds involve basic amino acids (R177, R186A, R186B and K187) and have occupancies above 80%. Remarkably Lys187 is involved in hydrogen bonds through its side chain (74.5%) and backbone (90.4%). We have earlier predicted, using simulations with an implicit membrane model and mutagenesis experiments [16], that R186A, R186B, K187 and R222 play a major role in PR3 interaction with cell membranes. In particular mutating these four amino acids into four alanines would abrogate PR3 membrane expression in Rat Basophil Leukemia (RBL) cells. Our

[4] PR3 and HNE amino acids are numbered according to the chymotrypsin convention which is common for all serine proteases of the family. To account for insertions this convention includes letters and numbers (Cf methods section)

results confirm the importance of this cluster of basic amino acids constituted of four arginines (R177, R186A, R186B, R222) and one lysine (K187). Besides these, lysine 99 (K99) reported to be important for ligand binding [48, 49] mediates hydrogen bonds with the lipids. It is also the case of F166 and W218 although they mediate interactions via their backbone atoms while their side chains are heavily involved in hydrophobic contacts with the lipid tails.

We calculated the average number of hydrophobic contacts per frame along the sampling window (Cf. Table 1). Several amino acids of the predicted interfacial binding site display hydrophobic contacts with the POPC lipid bilayer. As expected these are aromatic (F165, F166, W218, F224) and hydrophobic amino acids (V163, T221, L223 and P225). Among these, V163, F166, L223 have particularly high average number of contacts (2.3, 2.5 and 5.8, respectively). Simultaneous mutations of the four amino acids F165, F166, L223 and F224 did impair membrane expression of PR3 on RBL cells[16]. Interestingly the basic cluster involved in strong hydrogen bonding (R177, R186A, R186B, K187) is also involved in hydrophobic contacts with the lipid tails. In agreement with its involvement in hydrogen bonds with POPC glycerol groups, R186A is the basic amino acid with the higher number of hydrophobic contacts. The aromatic residues F165, F166, W218 and F224 are actually embedded in the bilayer.

While we observed strong cation-pi interactions between W218 and DMPC lipids in our previous work, the occupancy of this interaction is of only 5.7 % in the present simulation, which we do not consider as being significant.

3.1.2. HNE

Using an implicit membrane model, we previously predicted that HNE would bind to cell membranes using the same interfacial binding site as PR3[14]. We therefore inserted HNE in the POPC bilayer similarly to Proteinase 3; using the same orientation and the same depth of anchoring. With the implicit membrane model, we also observed a higher electrostatic contribution than in the case of PR3 and fewer contributions from hydrophobic amino acids.

The structure of HNE is unaffected by the POPC bilayer (RMSD 1.26±0.17 Å) and as PR3, it remains stably anchored at the bilayer interface (Cf. Supp Mat, Fig. S2) although a visual inspection of the trajectories indicate that the orientation of HNE with respect to the membrane plane varies more than that of PR3. Most of the interactions with POPC lipids are achieved by amino acids carried by the same three loops as in PR3 (β8-β9, β9-β10, β11-β12) (Cf Table 2) plus an additional interaction through R146 (loop β7-β8). In fact basic residues located on the loops β7-β8, β8-β9 and β9-β10 seem to alternate as anchors with the protein tilting around an axis perpendicular to the bilayer along the simulation. This is well illustrated by the variation along time of the depth of anchoring of amino acids R146 (β7-β8), R177, R178 (β8-β9) and R186 of loop β9-β10 (Cf fig S3 in Supplementary data). The proline and valine numbered 96 and 97, respectively (P96, V97, on loop β5-β6), are involved in interactions with the lipid tails as illustrated by their number of hydrophobic contacts (1.0 and 2.6, respectively. Cf Table 2). V97 is only two amino acids away from L99, which interestingly is not observed to interact with the lipids. Its equivalent in PR3 is a lysine (K99) and is observed to interact with the lipid heads via hydrogen bonds.

Hydrogen bonds between HNE and the lipids are mediated by more amino acids than in the case of PR3 (12 against 8) but only one out of the twelve, R178, has an

occupancy above 80%. R177 and R178 are the arginines that on average are the most deeply inserted into the interface during the simulation (Cf Table 2 and Fig.S3 in supplementary data).

Only five amino acids mediate an average number of hydrophobic contacts above or equal to 1.0 (V97, P96, L166, R177 and L223). This is strikingly less than in PR3 of which 12 amino acids had a higher number of hydrophobic contacts than this threshold. The two leucines mediate the highest number of contacts and L223 is the only residue anchored beyond the phosphate plane (Cf Table 2). Amino acids K99 of PR3 forms hydrogen bonds with POPC lipids (Cf previous paragraph), while it is not the case of its equivalent in HNE (L99) which cannot form hydrogen bonds; instead two other amino acids of the same loop (β5-β6, P96 and V97) mediate hydrophobic contacts with the lipids.

All together the simulation results indicate that HNE interacts with the bilayer using mostly hydrogen bonds and very few hydrophobic anchors, suggesting a looser binding to lipid membranes than PR3.

3.2 Surface Plasmon Resonance

To experimentally verify the hypotheses resulting from the MD simulations, we conducted SPR assays to compare the affinity of PR3 and HNE for large unilamellar vesicles (LUVs) constituted of POPC lipids.

Liposome immobilization.

Liposomes were immobilized on the surface of the L1 sensor chip at a low flow rate (1 $\mu L \cdot min^{-1}$) until the maximal amount of deposition was reached. Liposome immobilization levels were monitored over time and the mean immobilization level

for POPC LUVs was 8669 ± 95 RU calculated on four different experiments (Cf. Table 1). To avoid non-specific binding of proteins to the surface of the L1 chips, special care was taken to cover the chip surface at the highest possible levels of liposomes. The level of the coverage sensor chip was assessed with BSA injections (0.1 $mg \cdot ml^{-1}$). Resulting signals from BSA of around 100 RU or less indicate a sufficient coverage (Erb et al., 2000). In our case, BSA binding amounts to 43 ± 2 RUs and allowed us to pursue experiments further with POPC.

Binding of PR3 to POPC LUVs

We investigated the interaction of PR3 with neutral liposomes made of POPC using SPR. Liposomes were immobilized on the surface of the L1 sensor chip as described above. Binding assays were performed by injecting protein samples at increasing concentration and affinity calculations were carried out by steady state analysis. We monitored the association phase for 180 seconds and the dissociation phase for 420 seconds. The sensorgrams (Figure 4) show that the protein response is concentration dependent and is reaching equilibrium towards the end of each injection. The calculated K_d between PR3 and POPC is $9.22 \cdot 10^{-7}$ M. During the dissociation phase, we also observed that the response signal of PR3 does not return to zero and thus demonstrates a persistent binding of PR3 to the liposomes.

Binding of HNE to POPC LUVs

The binding of HNE towards POPC was monitored using the same procedure as for PR3. The association of the protein to the LUVs was monitored for 120 s (shorter than for PR3) and the dissociation for 420 s. The sensorgrams are presented on Figure 2B and show that HNE can bind to liposomes made of POPC in a concentration-

dependent manner which indicates a direct binding of the protein to the liposomes. During the dissociation phase, the signal drops immediately and returns to the baseline value. This is in contrast to the behavior of PR3. The kinetics of the protein-membrane interaction seems to be different for the two proteins. For the K_d calculation, the data collected for HNE clearly show that equilibrium was not reached even at 3 μM. It was therefore not possible to calculate the affinity accurately but we can evaluate a lower limit for the K_d value of $3.4 \cdot 10^{-6}$ M.

4. DISCUSSION AND CONCLUSION

The SPR experiments yield a K_d in the low micromolar range ($9.22 \pm 0.4 \cdot 10^{-7}$ M) for PR3, while the binding of HNE is weaker and its K_d is not within the range of concentrations tested. For comparison, K_d measured for hIIa-PLA_2 with the same method was $6.8\ 10^{-8}$ M [25] and for the lactadehrin C2 domain $3.2\ 10^{-7}$ M [50]. The difference we observe between PR3 and HNE is consistent with the results of Goldman et al. although we measure a K_d for PR3 with POPC that is lower by two orders of magnitude than the value they determined in 1999 ($85 \cdot 10^{-6}$ M) using spectrophotometric measurements and DMPC vesicles. Both our choice of method and lipids may have influenced the results; bilayers of POPC have a T_m of -2°C and DMPC has a T_m of +23°C. Moreover, their study appears to have been conducted using multilamellar vesicles, whereas ours were extruded to produce monodisperse unilamellar vesicles.

Although the use of a low flow rate for the injection of protein on the SPR chip prevents us from determining accurate rate constants, the SPR sensorgrams show significantly different dissociation rates for PR3 and HNE, indicating that both enzymes are bound differently to the lipid bilayer with PR3 binding being perpetuated

after the flow is interrupted, while HNE transfers back to the bulk almost immediately. Generally, long-range non-specific interactions (typically electrostatics) accelerate the association of peripheral membrane protein and short range interactions (typically Van der Waals) slow the dissociation[51]. While our SPR sensorgrams show no visible differences in the association phase, they clearly show a slower dissociation for PR3, which would therefore imply that short-range interactions are lacking in HNE. The difference between PR3 and HNE in terms of short range van der Waals interactions is clearly characterized by our MD simulations. The IBS for HNE and PR3 are different (Tables 1 and 2, Fig.3) leading to a higher average number of hydrophobic contacts per simulation frame between the lipids and PR3 (27.1) than between the lipids and HNE (16.9). On the other hand, and although both HNE and PR3 have about the same number of basic amino acids at their IBS, HNE achieves a higher number of hydrogen bonds with the lipid phosphates. Particularly relevant to the difference in dissociation rates is the fact that PR3 inserts a higher number of aromatic amino acids (F165, F166, W218, F224 in PR3 vs. F192 in HNE) below the plane of the phosphorus atoms. This may also explain the higher shift in the membrane transition temperature observed for PR3 vs HNE by differential scanning calorimetry in the study from Goldman et al. According to the Wimley-White interfacial hydrophobicity scale, based on the transfer free energy of pentapeptides (AcWL-X-LL) from water to a POPC bilayer[52, 53], aromatic residues have the most favourable partitioning energies, while charged amino acids have large unfavourable energies. Other amino acids make relatively small contributions. The difference in the number of aromatic residues inserted by both enzymes in the bilayer thus explains the difference in membrane affinity for PR3 and HNE.

Peripheral membrane proteins bind reversibly to biological membranes and it is generally acknowledged that electrostatic interactions drive their positioning and orientation at the membrane surface thus facilitating the intercalation of a few hydrophobic groups [54]. While the association of amphitropic proteins with lipid bilayers is fast their dissociation is generally slow [25, 51] with the dissociation rate being the main determinant of the binding strength. As a consequence, in simple systems where the protein does not undergo conformational changes and does not interact with other proteins, the affinity for the membrane is mostly accounted for by interactions between the protein interfacial binding site and lipids.

The SPR sensorgrams and the difference in the number of hydrophobic and aromatic amino acids anchored in the hydrophobic region of the bilayer between both enzymes is thus consistent with a specific association of PR3 to the plasma membrane, "*stronger than only an ionic interaction*"[11] with insertion of hydrophobic amino acids (Hajjar et al. Proteins) while HNE has a more shallow electrostatic interaction with LUVs. The SPR experiments also correlate well with simulations using an implicit membrane model [14] predicting strong electrostatic contribution in the binding of HNE to lipid bilayers.

Using long molecular dynamics simulations of PR3 at the surface of POPC bilayers and SPR experiments following the binding of PR3 to POPC LUVS, we have demonstrated that PR3 can bind directly to lipid bilayers by inserting one aliphatic and four aromatic amino acids into the hydrophobic core of the bilayer. HNE interacts with the same LUVs in a shallower manner dominated by electrostatic interactions. The difference in affinity between the two proteins can be explained by the difference in the nature of their IBS, namely the number of aromatic amino acids present.

Our results thus indicate that PR3 has direct interactions with the neutrophil membrane, which is mostly constituted of POPC lipids and does not require a transmembrane protein as receptor to be present at the neutrophil surface. We however do not exclude the existence of partner proteins to membrane-bound PR3 membrane binding as these are likely to stabilize the membrane bound protease and will be necessary for it to achieve its function.

ACKNOWLEDGEMENTS

This work was supported by grants from the Bergen Research Foundation and the Norwegian Research Council. Parallab (High Performance Computing Laboratory at the University of Bergen) and NOTUR (Norwegian metacenter for computational science) are thankfully acknowledged for provision of CPU time.

REFERENCES

[1] C. Nathan, Neutrophils and immunity: challenges and opportunities, Nat Rev Immunol, 6 (2006) 173-182.
[2] B. Amulic, C. Cazalet, G.L. Hayes, K.D. Metzler, A. Zychlinsky, Neutrophil function: from mechanisms to disease, Annual review of immunology, 30 (2012) 459-489.
[3] B. Korkmaz, M.S. Horwitz, D.E. Jenne, F. Gauthier, Neutrophil elastase, proteinase 3, and cathepsin G as therapeutic targets in human diseases, Pharmacol Rev, 62 (2010) 726-759.
[4] E. Hajjar, T. Broemstrup, C. Kantari, V. Witko-Sarsat, N. Reuter, Structures of human proteinase 3 and neutrophil elastase--so similar yet so different, The FEBS journal, 277 (2010) 2238-2254.
[5] E. Csernok, M. Ernst, W. Schmitt, D.F. Bainton, W.L. Gross, Activated neutrophils express proteinase 3 on their plasma membrane in vitro and in vivo., Clin Exp Immunol, 95 (1994) 244-250.
[6] V. Witko-Sarsat, P. Lesavre, S. Lopez, G. Bessou, C. Hieblot, B. Prum, L.H. Noel, L. Guillevin, P. Ravaud, I. Sermet-Gaudelus, J. Timsit, J.P. Grunfeld, L. Halbwachs-Mecarelli, A large subset of neutrophils expressing membrane proteinase 3 is a risk factor for vasculitis and rheumatoid arthritis, J Am Soc Nephrol, 10 (1999) 1224-1233.
[7] A.A. Rarok, C.A. Stegeman, P.C. Limburg, C.G. Kallenberg, Neutrophil membrane expression of proteinase 3 (PR3) is related to relapse in PR3-ANCA-associated vasculitis, J Am Soc Nephrol, 13 (2002) 2232-2238.
[8] A. Schreiber, A. Busjahn, F.C. Luft, R. Kettritz, Membrane expression of proteinase 3 is genetically determined, J Am Soc Nephrol, 14 (2003) 68-75.
[9] V. Witko-Sarsat, N. Reuter, L. Mouthon, Interaction of proteinase 3 with its associated partners: implications in the pathogenesis of Wegener's granulomatosis, Curr Opin Rheumatol, 22 (2010) 1-7.
[10] A. Schreiber, F.C. Luft, R. Kettritz, Membrane proteinase 3 expression and ANCA-induced neutrophil activation, Kidney Int, 65 (2004) 2172-2183.
[11] V. Witko-Sarsat, E.M. Cramer, C. Hieblot, J. Guichard, P. Nusbaum, S. Lopez, P. Lesavre, L. Halbwachs-Mecarelli, Presence of proteinase 3 in secretory vesicles: evidence of a novel, highly mobilizable intracellular pool distinct from azurophil granules, Blood, 94 (1999) 2487-2496.
[12] E.J. Campbell, M.A. Campbell, C.A. Owen, Bioactive proteinase 3 on the cell surface of human neutrophils: quantification, catalytic activity, and susceptibility to inhibition, J Immunol, 165 (2000) 3366-3374.
[13] W.H. Goldmann, J.L. Niles, M.A. Arnaout, Interaction of purified human proteinase 3 (PR3) with reconstituted lipid bilayers, Eur J Biochem, 261 (1999) 155-162.
[14] E. Hajjar, M. Mihajlovic, V. Witko-Sarsat, T. Lazaridis, N. Reuter, Computational prediction of the binding site of proteinase 3 to the plasma membrane, Proteins, 71 (2008) 1655-1669.
[15] T. Broemstrup, N. Reuter, How does proteinase 3 interact with lipid bilayers?, Phys Chem Chem Phys, 12 (2010) 7487-7496.
[16] C. Kantari, A. Millet, J. Gabillet, E. Hajjar, T. Broemstrup, P. Pluta, N. Reuter, V. Witko-Sarsat, Molecular analysis of the membrane insertion domain of proteinase 3, the Wegener's autoantigen, in RBL cells: implication for its pathogenic activity, J Leukoc Biol, 90 (2011) 941-950.

[17] N. Hu, J. Westra, C.G. Kallenberg, Membrane-bound proteinase 3 and its receptors: relevance for the pathogenesis of Wegener's Granulomatosis, Autoimmun Rev, 8 (2009) 510-514.
[18] S. von Vietinghoff, G. Tunnemann, C. Eulenberg, M. Wellner, M.C. Cardoso, F.C. Luft, R. Kettritz, NB1 mediates surface expression of the ANCA antigen proteinase 3 on human neutrophils, Blood, (2007).
[19] A. David, R. Fridlich, I. Aviram, The presence of membrane Proteinase 3 in neutrophil lipid rafts and its colocalization with FcgammaRIIIb and cytochrome b558, Exp Cell Res, 308 (2005) 156-165.
[20] A. David, Y. Kacher, U. Specks, I. Aviram, Interaction of proteinase 3 with CD11b/CD18 (beta2 integrin) on the cell membrane of human neutrophils, J Leukoc Biol, 74 (2003) 551-557.
[21] B. Jiang, E. Grage-Griebenow, E. Csernok, K. Butherus, S. Ehlers, W.L. Gross, J.U. Holle, The role of proteinase 3 (PR3) and the protease-activated receptor-2 (PAR-2) pathway in dendritic cell (DC) maturation of human-DC-like monocytes and murine DC, Clin Exp Rheumatol, 28 (2010) 56-61.
[22] C.J. Kuckleburg, P.J. Newman, Neutrophil proteinase 3 acts on protease-activated receptor-2 to enhance vascular endothelial cell barrier function., Arteriosclerosis, thrombosis, and vascular biology, 33 (2013) 275-284.
[23] C. Kantari, M. Pederzoli-Ribeil, O. Amir-Moazami, V. Gausson-Dorey, I.C. Moura, M.C. Lecomte, M. Benhamou, V. Witko-Sarsat, Proteinase 3, the Wegener autoantigen, is externalized during neutrophil apoptosis: evidence for a functional association with phospholipid scramblase 1 and interference with macrophage phagocytosis, Blood, 110 (2007) 4086-4095.
[24] B. Korkmaz, A. Kuhl, B. Bayat, S. Santoso, D.E. Jenne, A hydrophobic patch on proteinase 3, the target of autoantibodies in Wegener granulomatosis, mediates membrane binding via NB1 receptors, J Biol Chem, 283 (2008) 35976-35982.
[25] R. Stahelin, W. Cho, Differential roles of ionic, aliphatic, and aromatic residues in membrane-protein interactions: a surface plasmon resonance study on phospholipases A2, Biochemistry, 40 (2001) 4672-4678.
[26] R.V. Stahelin, Surface plasmon resonance: a useful technique for cell biologists to characterize biomolecular interactions., Molecular biology of the cell, 24 (2013) 883-886.
[27] S. Jaud, D.J. Tobias, J.J. Falke, S.H. White, Self-induced docking site of a deeply embedded peripheral membrane protein, Biophys J, 92 (2007) 517-524.
[28] B. Rogaski, J.B. Klauda, Membrane-binding mechanism of a peripheral membrane protein through microsecond molecular dynamics simulations, J Mol Biol, 423 (2012) 847-861.
[29] C.N. Lumb, J. He, Y. Xue, P.J. Stansfeld, R.V. Stahelin, T.G. Kutateladze, M.S. Sansom, Biophysical and computational studies of membrane penetration by the GRP1 pleckstrin homology domain, Structure, 19 (2011) 1338-1346.
[30] S. Jo, T. Kim, V.G. Iyer, W. Im, CHARMM-GUI: a web-based graphical user interface for CHARMM, J Comput Chem, 29 (2008) 1859-1865.
[31] J.C. Phillips, R. Braun, W. Wang, J. Gumbart, E. Tajkhorshid, E. Villa, C. Chipot, R.D. Skeel, L. Kale, K. Schulten, Scalable molecular dynamics with NAMD, J Comput Chem, 26 (2005) 1781-1802.
[32] J.B. Klauda, R.M. Venable, J.A. Freites, J.W. O'Connor, D.J. Tobias, C. Mondragon-Ramirez, I. Vorobyov, A.D. MacKerell, Jr., R.W. Pastor, Update of the CHARMM all-atom additive force field for lipids: validation on six lipid types, J Phys Chem B, 114 (2010) 7830-7843.

[33] H.C. Andersen, Rattle - a Velocity Version of the Shake Algorithm for Molecular-Dynamics Calculations, J. Comp. Phys., 52 (1983) 24-34.
[34] T. Darden, D. York, L. Pedersen, Particle Mesh Ewald - an N.Log(N) Method for Ewald Sums in Large Systems, J Chem Phys, 98 (1993) 10089-10092.
[35] U. Essmann, L. Perera, M.L. Berkowitz, T. Darden, H. Lee, L.G. Pedersen, A smooth particle mesh Ewald method, J Chem Phys, 103 (1995) 8577-8593.
[36] S.E. Feller, Y.H. Zhang, R.W. Pastor, B.R. Brooks, Constant-Pressure Molecular-Dynamics Simulation - the Langevin Piston Method, J Chem Phys, 103 (1995) 4613-4621.
[37] W. Humphrey, A. Dalke, K. Schulten, VMD - Visual Molecular Dynamics, J. Molec. Graphics, 14 (1996) 33-38.
[38] N. Kucerka, S. Tristram-Nagle, J.F. Nagle, Structure of fully hydrated fluid phase lipid bilayers with monounsaturated chains., The Journal of membrane biology, 208 (2005) 193-202.
[39] M. Fujinaga, M.M. Chernaia, R. Halenbeck, K. Koths, M.N. James, The crystal structure of PR3, a neutrophil serine proteinase antigen of Wegener's granulomatosis antibodies, J Mol Biol, 261 (1996) 267-278.
[40] H.M. Berman, J. Westbrook, Z. Feng, G. Gilliland, T.N. Bhat, H. Weissig, I.N. Shindyalov, P.E. Bourne, The Protein Data Bank, Nucleic Acids Res, 28 (2000) 235-242.
[41] W. Bode, A. Wei, R. Huber, E. Meyer, J. Travis, S. Neumann, X-ray crystal structure of the complex of human leukocyte elastase (PMN elastase) and the third domain of the turkey ovomucoid inhibitor., EMBO J, 5 (1986) 2453-2458.
[42] B.R. Brooks, C.L. Brooks, 3rd, A.D. Mackerell, Jr., L. Nilsson, R.J. Petrella, B. Roux, Y. Won, G. Archontis, C. Bartels, S. Boresch, A. Caflisch, L. Caves, Q. Cui, A.R. Dinner, M. Feig, S. Fischer, J. Gao, M. Hodoscek, W. Im, K. Kuczera, T. Lazaridis, J. Ma, V. Ovchinnikov, E. Paci, R.W. Pastor, C.B. Post, J.Z. Pu, M. Schaefer, B. Tidor, R.M. Venable, H.L. Woodcock, X. Wu, W. Yang, D.M. York, M. Karplus, CHARMM: the biomolecular simulation program, J Comput Chem, 30 (2009) 1545-1614.
[43] A.D. MacKerell, D. Bashford, M. Bellott, R.L. Dunbrack, J.D. Evanseck, M.J. Field, S. Fischer, J. Gao, H. Guo, S. Ha, D. Joseph-McCarthy, L. Kuchnir, K. Kuczera, F.T.K. Lau, C. Mattos, S. Michnick, T. Ngo, D.T. Nguyen, B. Prodhom, W.E. Reiher, B. Roux, M. Schlenkrich, J.C. Smith, R. Stote, J. Straub, M. Watanabe, J. Wiorkiewicz-Kuczera, D. Yin, M. Karplus, All-atom empirical potential for molecular modeling and dynamics studies of proteins, Journal of Physical Chemistry B, 102 (1998) 3586-3616.
[44] J.A. Izaguirre, S. Reich, R.D. Skeel, Longer time steps for molecular dynamics, J Chem Phys, 110 (1999) 9853-9864.
[45] C. Grauffel, B. Yang, T. He, M.F. Roberts, A. Gershenson, N. Reuter, Cation-pi interactions as lipid-specific anchors for phosphatidylinositol-specific phospholipase C, J Am Chem Soc, 135 (2013) 5740-5750.
[46] R. Mouri, K. Konoki, N. Matsumori, T. Oishi, M. Murata, Complex Formation of Amphotericin B in Sterol-Containing Membranes As Evidenced by Surface Plasmon Resonance†, Biochemistry, 47 (2008) 7807-7815.
[47] A. Olaru, M. Gheorghiu, S. David, C. Polonschii, E. Gheorghiu, Quality assessment of SPR sensor chips; case study on L1 chips, Biosensors & bioelectronics, 45 (2013) 77-81.

[48] E. Hajjar, B. Korkmaz, F. Gauthier, B.O. Brandsdal, V. Witko-Sarsat, N. Reuter, Inspection of the binding sites of proteinase3 for the design of a highly specific substrate, J Med Chem, 49 (2006) 1248-1260.
[49] S. Narawane, A. Budnjo, C. Grauffel, B.E. Haug, N. Reuter, In Silico Design, Synthesis, and Assays of Specific Substrates for Proteinase 3: Influence of Fluorogenic and Charged Groups, J Med Chem, (2014).
[50] R.V. Stahelin, Surface plasmon resonance: a useful technique for cell biologists to characterize biomolecular interactions, Molecular biology of the cell, 24 (2013) 883-886.
[51] W. Cho, R.V. Stahelin, Membrane-protein interactions in cell signaling and membrane trafficking, Annual review of biophysics and biomolecular structure, 34 (2005) 119-151.
[52] S.H. White, W.C. Wimley, Hydrophobic interactions of peptides with membrane interfaces, Biochim Biophys Acta, 1376 (1998) 339-352.
[53] W.C. Wimley, S.H. White, Experimentally determined hydrophobicity scale for proteins at membrane interfaces, Nat Struct Biol, 3 (1996) 842-848.
[54] O. Halskau, N.A. Froystein, A. Muga, A. Martinez, The membrane-bound conformation of alpha-lactalbumin studied by NMR-monitored 1H exchange, J Mol Biol, 321 (2002) 99-110.

FIGURE CAPTIONS

Figure 1: Sequence alignment of PR3 and HNE. The two sequences share 56% sequence identity. We use boxes to highlight amino acids of HNE corresponding to the predicted PR3 IBS (blue fonts for basic residues and orange for hydrophobic amino acids). Amino acids forming the catalytic triad are labeled with green fonts.

Figure 2: (A) Structural alignment of PR3 (grey) and HNE (green). The proteins secondary structure elements are represented using cartoons while each amino acid forming the PR3 IBS, as well as the corresponding amino acid in HNE, are represented using a ball (blue and orange for basic and hydrophobic amino acids, respectively, green for others). The nature of these amino acids in PR3 and HNE is shown on panels (B) and (C), respectively.

Figure 3: Molecular dynamics simulations of PR3 and HNE at the surface of a POPC bilayer. (A) Simulated system with HNE represented using green cartoons, the POPC bilayer using sticks colored by atom types and the water molecules in light blue. Randomly picked snapshots of the (B) PR3 and (C) HNE interface binding sites (286 and 343 ns, respectively). Amino acids mediating either hydrogen bonds of at least 45 % occupancy for hydrogen bonds or at least one hydrophobic contact on average, are highlighted with balls.

Figure 4: Binding assay of PR3 and HNE to LUVs from Surface Plasmon Resonance. PR3 (A) and HNE (B) binding responses, and respective affinity data below (C. PR3 and D. HNE) over immobilized POPC. All data are blank subtracted. No double referencing has been done due to high non specific binding to the reference channel (L1 chip with no liposomes – data not shown).

TABLES

Table 1. Anchorage of PR3 in a POPC lipid bilayer: inventory of interactions and depth of anchorage.

Loop	**Amino acid**	Depth[a] (Å)	Hydrophobic contacts[b]	Hydrogen bonds[c] (%)	Cation-π[e] (%)
β5-β6	**K99**	- 11.2 ± 2.8		20.1	
β8-β9	**V163**	- 3.0 ± 1.9	2.3		
	T164	- 2.8 ± 2.0		45.6	
	F165	+ 1.3 ± 1.8	1.5		
	F166	+ 1.7 ± 1.7	2.5	**28.1**	
	R177	- 4.8 ± 2.5	1.1	87.9	
β9-β10	**R186A**	+ 0.0 ± 2.3	4.2	85.9	
	R186B	- 2.2 ± 2.7	1.5	58.7[d]/82.9	
	K187	- 1.2 ± 2.4	1.6	**90.4**/74.5	
β11-β12	**F215**	- 10.0 ± 2.2			5.9
	W218	+ 0.8 ± 2.8	1.9	**26.6**	5.7
	T221	- 0.9 ± 2.4	1.6		
	R222	-0.2 ± 2.0		49.0[d]	
	L223	+ 2.5 ± 2.2	5.8		
	F224	+ 0.3 ± 1.8	1.2		
	P225	- 2.0 ± 1.6	1.9		

[a] Positive values indicate that the center of mass of the amino acid is buried in the bilayer beyond the plane defined by the phosphate groups. [b] Average number of hydrophobic contacts per frame (listed if above 1). [c] Occupancies of hydrogen bonds with POPC phosphate groups in % (if > 20; bold numbers are for hydrogen bonds involving the protein backbone) . [d] Hydrogen bond between Arg186B or Arg222 and POPC glycerols. [e] Occupancy of cation-π adducts (if > 5%).

Table 2. Anchorage of HNE in a POPC lipid bilayer: inventory of interactions and depth of anchorage.

Loop	**Amino acid**	Depth[a] (Å)	Hydrophobic contacts[b]	Hydrogen bonds[c] (%)	Cation-π[e] (%)
β5-β6	**P96**	-7.2± 5.8	1.0		
	V97	-3.8± 5.3	2.6		
β7-β8	**R146**	-9.4 ± 2.5		69.0	
β8-β9	**T164**	-5.7 ± 2.7		25.8	
	S165	-2.9 ± 2.5		36.0	
	L166	-0.6 ± 2.1	5.9	25.4	
	R177	-4.3 ± 3.1	1.1	64.8	
	R178	-4.3 ± 3.2		**23.2**/84.9	
β9-β10	**R186**	-6.7± 3.8		62.2/20.2[d]	
	G186A	-6.9 ± 3.5		**41.7**	
	F192	-11.6 ± 3.8			13.2
β11-β12	**R217**	-7.2 ± 4.4		49.0	
	S221	-3.2 ± 2.4		28.0	
	G222	-2.6 ± 2.1		**28.4**	
	L223	+0.4 ± 2.0	6.3		
	Y224	-1.3 ± 1.9		31.1[d]	

[a] Mean values and standard deviations. Positive values indicate that the center of mass of the amino acid is buried in the bilayer beyond the plane defined by the phosphate groups. [b] Average number of hydrophobic contacts per frame (listed if above 1). [c] Occupancies of hydrogen bonds in % (occupancies less than 20% are omitted; bold numbers for backbone hydrogen bonds). [d] Hydrogen bond between R186 or Y224 and POPC glycerols. [e] Occupancy of cation-π adducts (occupancies less than 5% are omitted).

Table 3: LUVs immobilization levels and chip coverage accession by BSA binding (BSA is used at 0.1 mg/ml and is injected 60 s at 60 $l.min^{-1}$). Values reported are the means and standard deviations of four experiments.

Immobilization level (RU)	BSA binding level (RU)
8669 ± 95	43 ± 2.6

Table 4: K_d values for PR3 and HNE with POPC LUVs. Values reported are the means and standard deviations of six experiments for PR3 and four for HNE.

K_d ($x10^{-7}$ M)	
PR3	HNE
9.22 ± 0.4	> 33.4 ± 4

HIGHLIGHTS

- Proteinase 3 binds directly and strongly to lipid vesicles ($K_d = 9.2 \cdot 10^{-7}$ M)

- PR3 binds to lipid vesicles with a higher affinity than its homologue HNE does

- Four aromatic amino acids contribute the affinity difference between PR3 and HNE

Figure 1

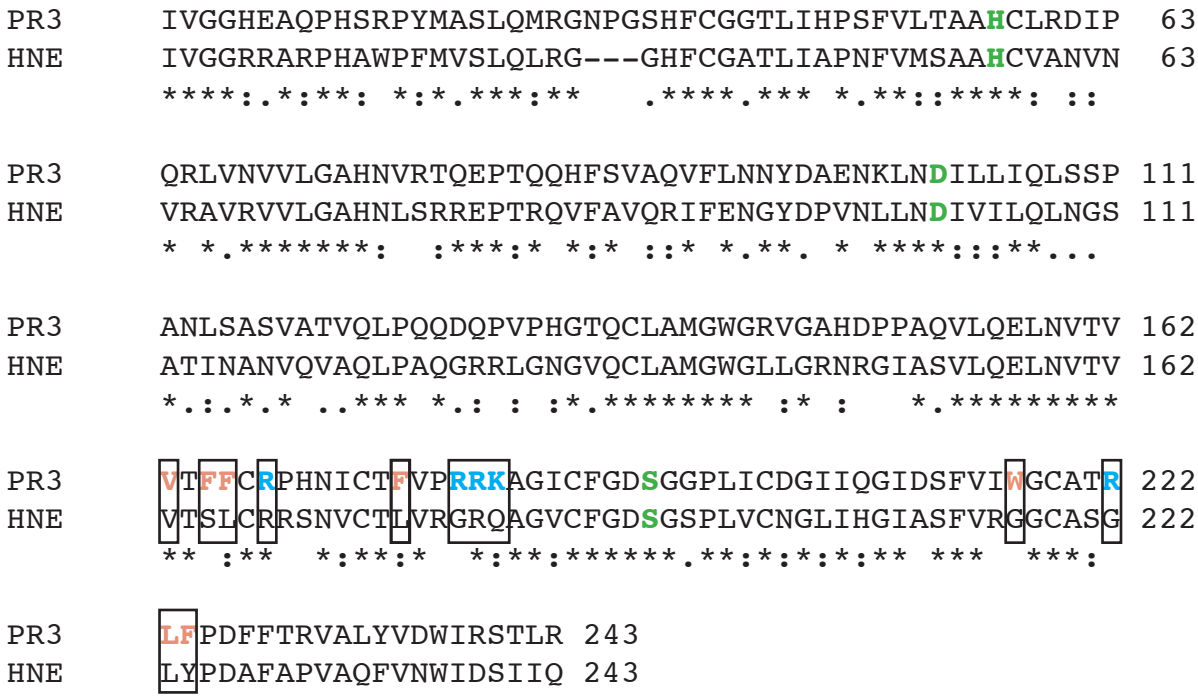
PR3 IVGGHEAQPHSRPYMASLQMRGNPGSHFCGGTLIHPSFVLTAAHCLRDIP 63
HNE IVGGRRARPHAWPFMVSLQLRG---GHFCGATLIAPNFVMSAAHCVANVN 63
PR3 QRLVNVVLGAHNVRTQEPTQQHFSVAQVFLNNYDAENKLNDILLIQLSSP 111
HNE VRAVRVVLGAHNLSRREPTRQVFAVQRIFENGYDPVNLLNDIVILQLNGS 111
PR3 ANLSASVATVQLPQQDQPVPHGTQCLAMGWGRVGAHDPPAQVLQELNVTV 162
HNE ATINANVQVAQLPAQGRRLGNGVQCLAMGWGLLGRNRGIASVLQELNVTV 162
PR3 VTFFCRPHNICTFVPRRKAGICFGDSGGPLICDGIIQGIDSFVIWGCATR 222
HNE VTSLCRRSNVCTLVRGRQAGVCFGDSGSPLVCNGLIHGIASFVRGGCASG 222
PR3 LFPDFFTRVALYVDWIRSTLR 243
HNE LYPDAFAPVAQFVNWIDSIIQ 243

Figure 2A

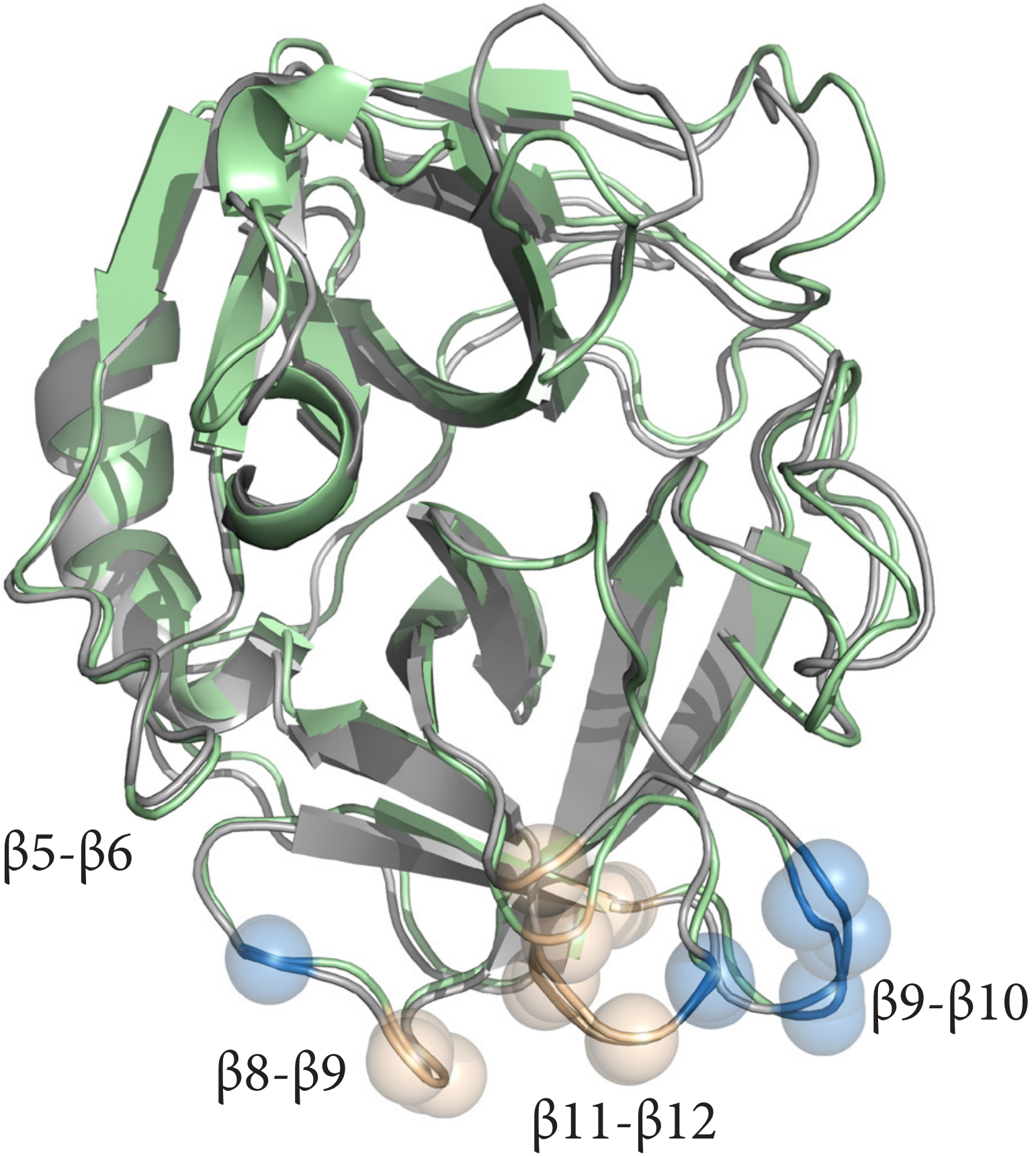

Figure 2B

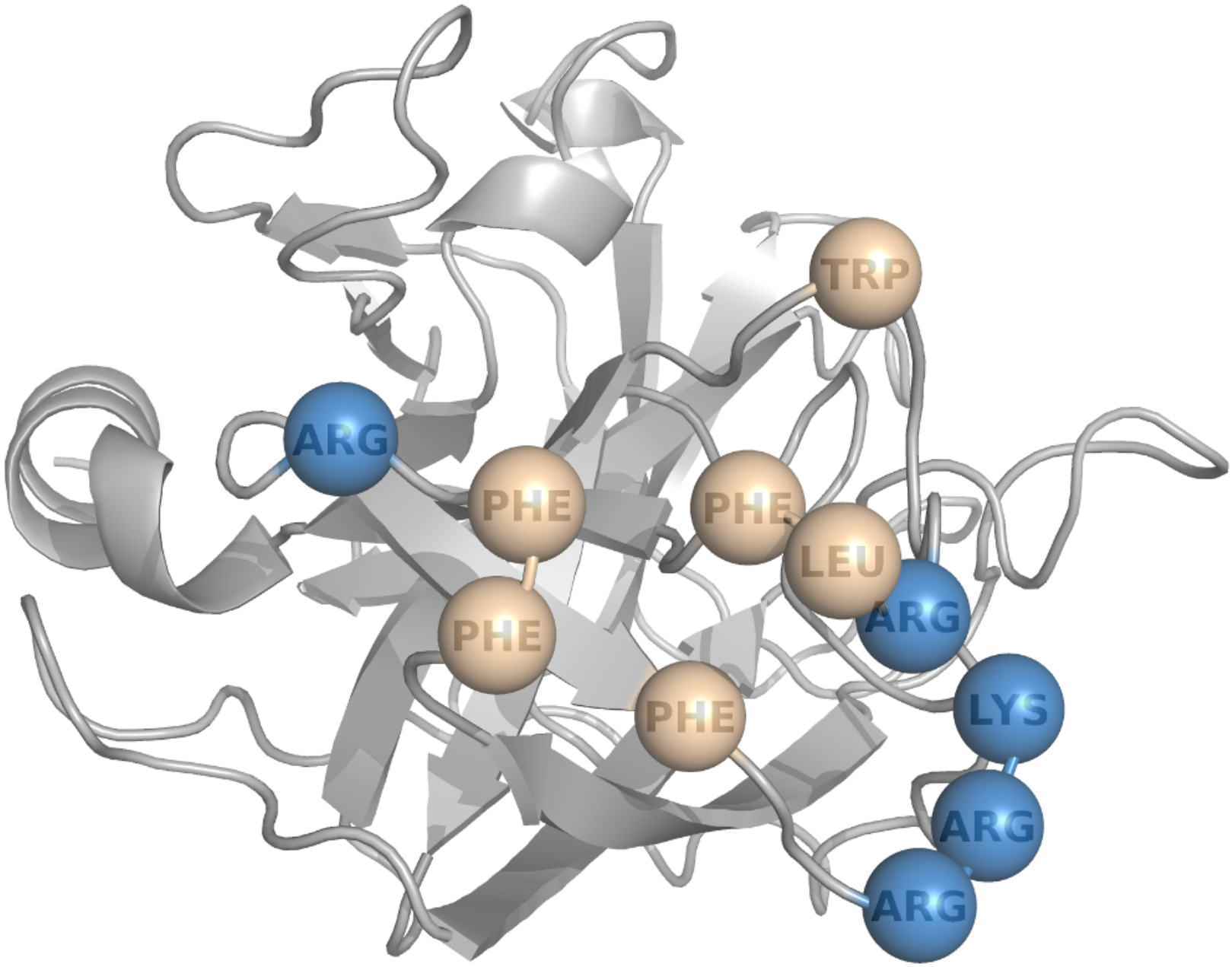

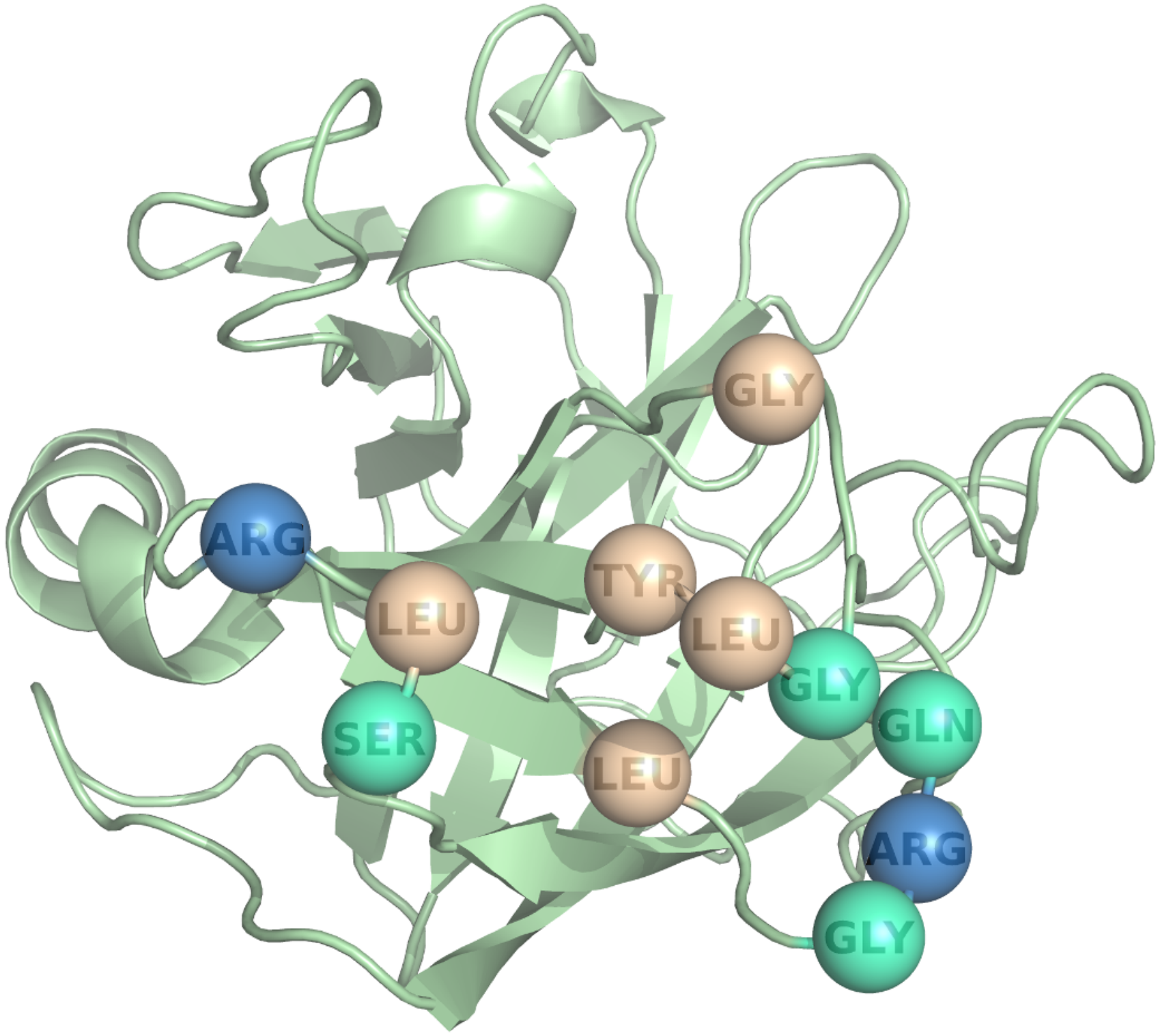
GLY
ARG
TYR
LEU
LEU
GLY
GLN
SER
LEU
ARG
GLY

Figure 3A

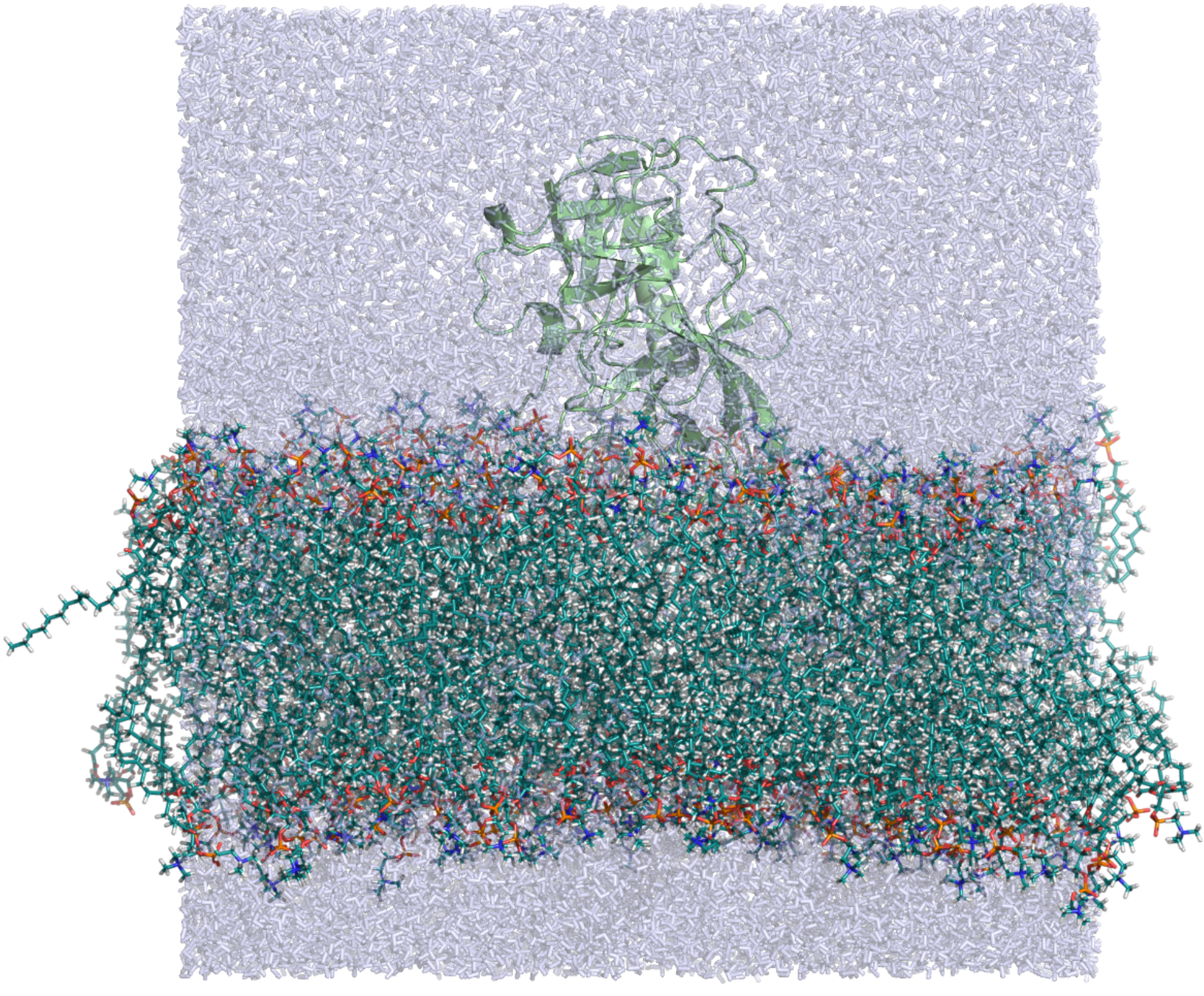

Figure 3B

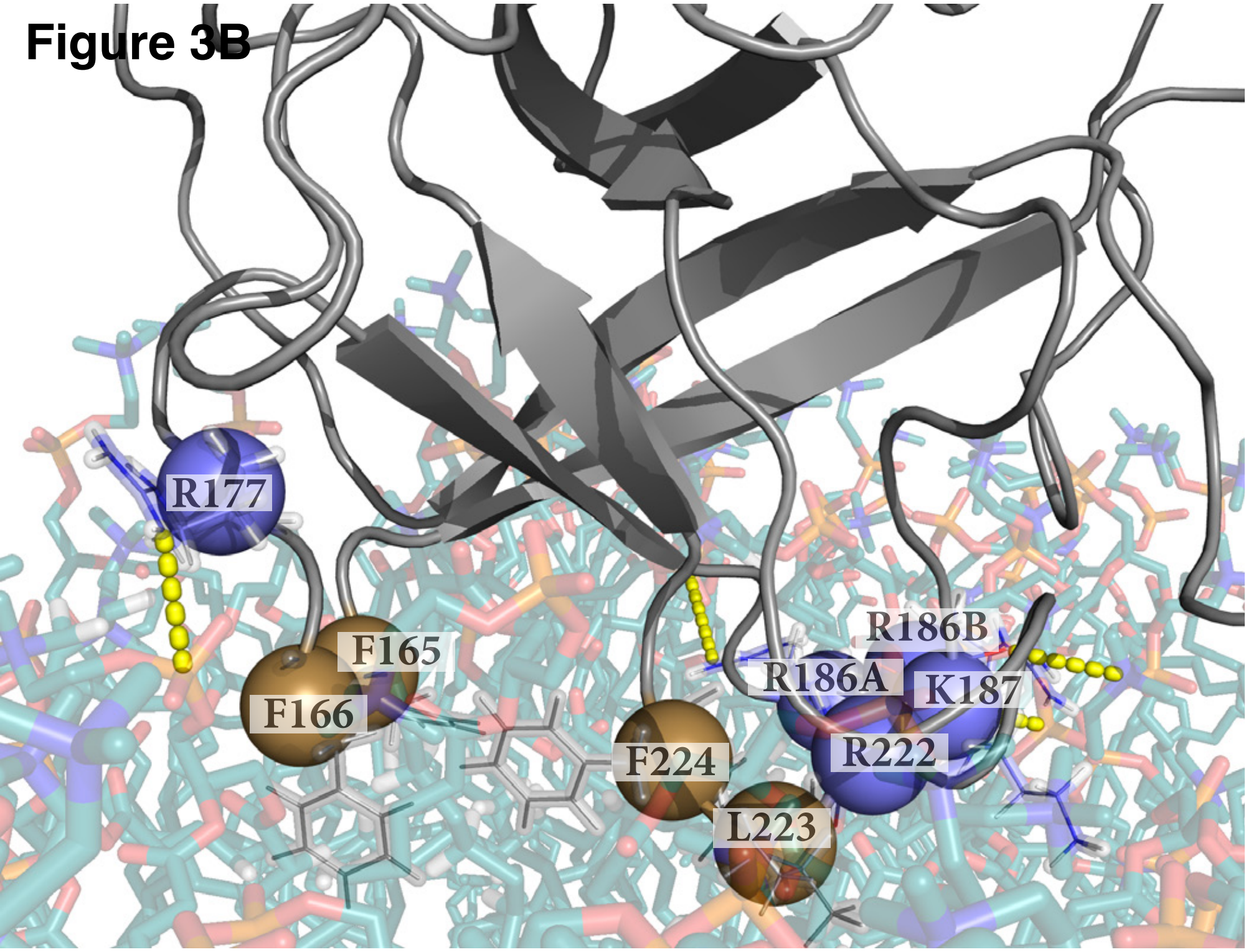

Figure 3C

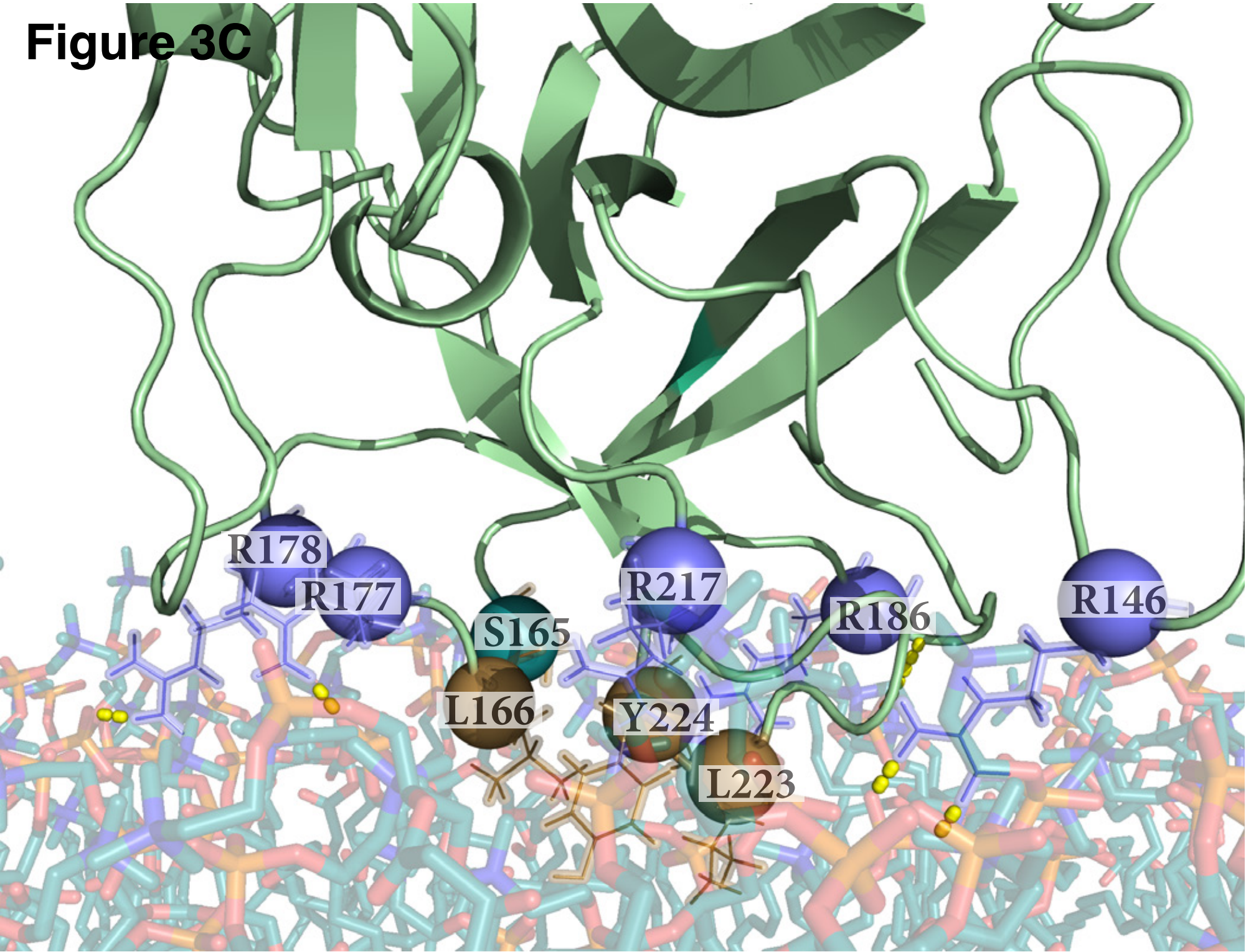

Figure4A

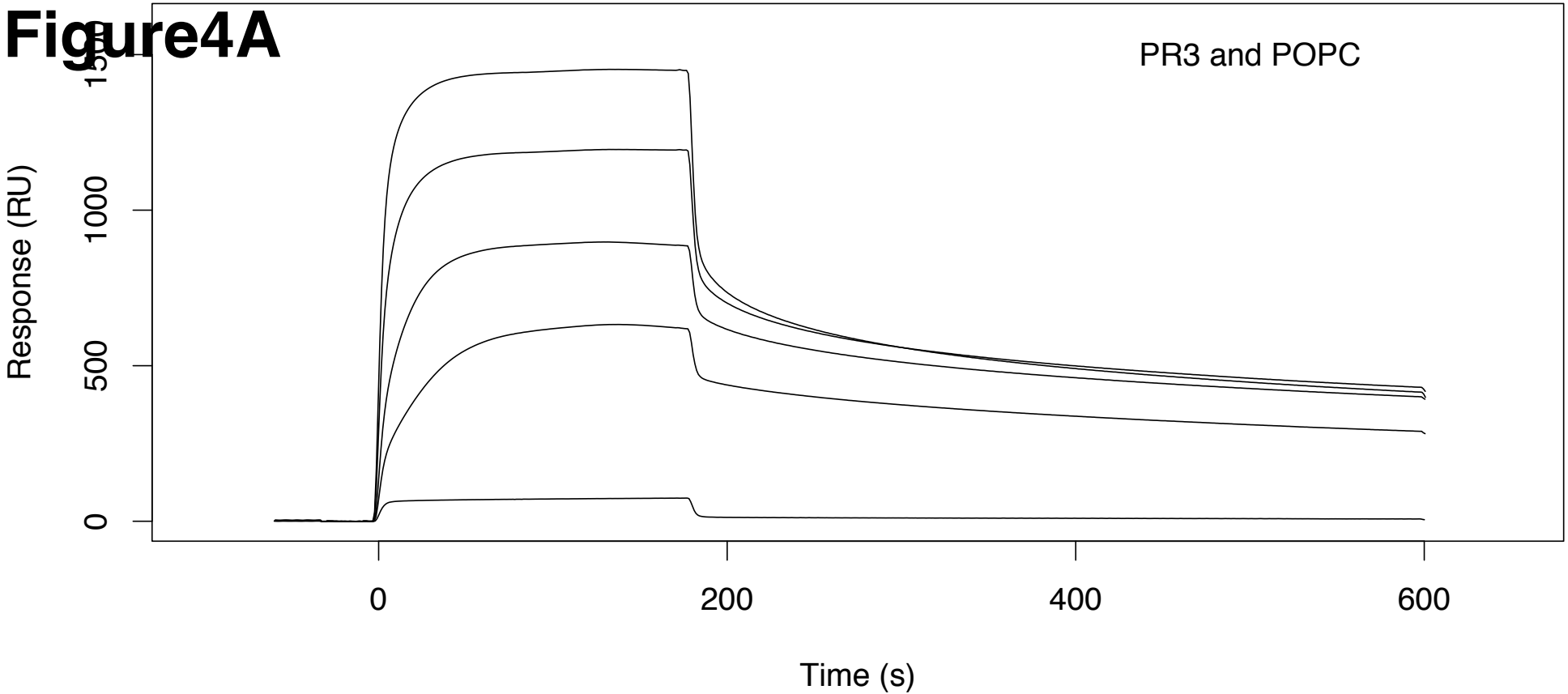

Figure4B

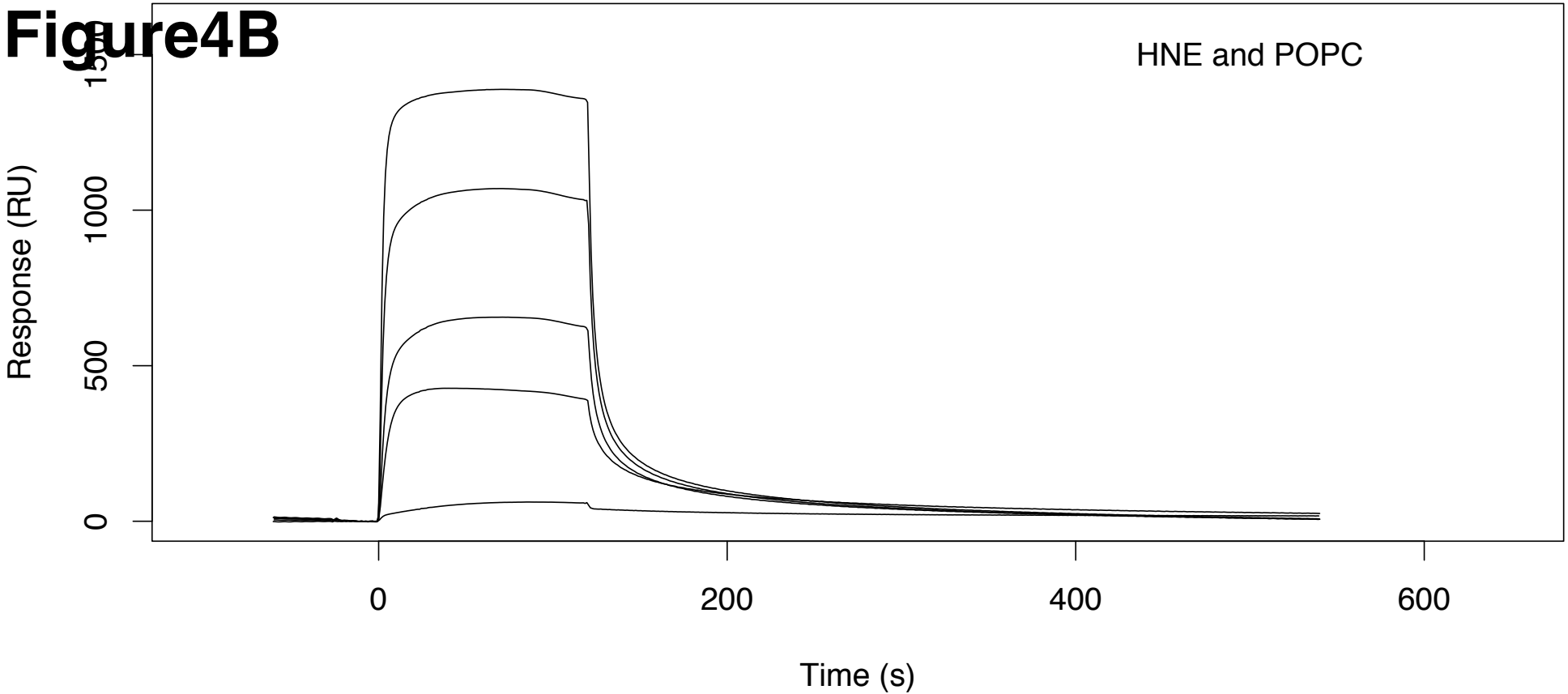

Figure4C

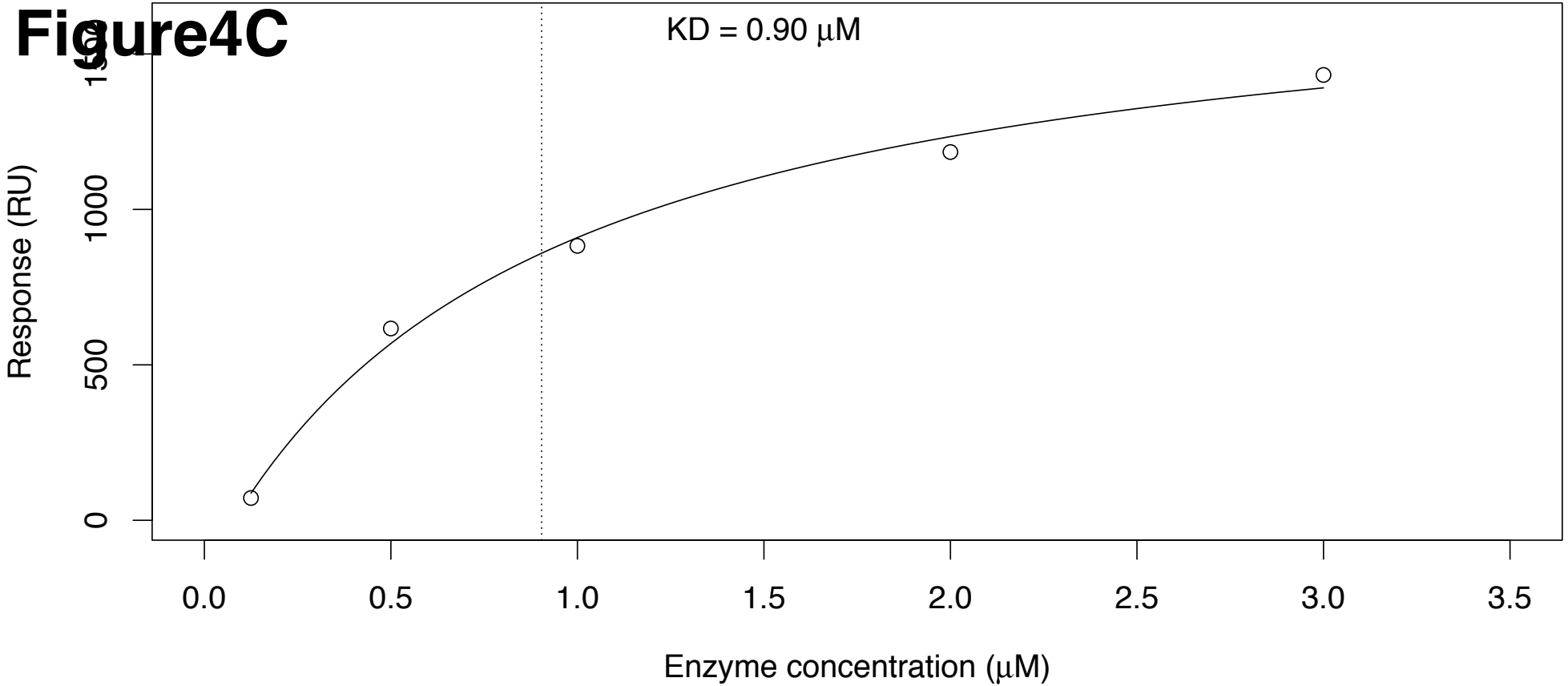
KD = 0.90 μM
Response (RU)
0
500
1000
0.0
0.5
1.0
1.5
2.0
2.5
3.0
3.5
Enzyme concentration (μM)

Figure4D

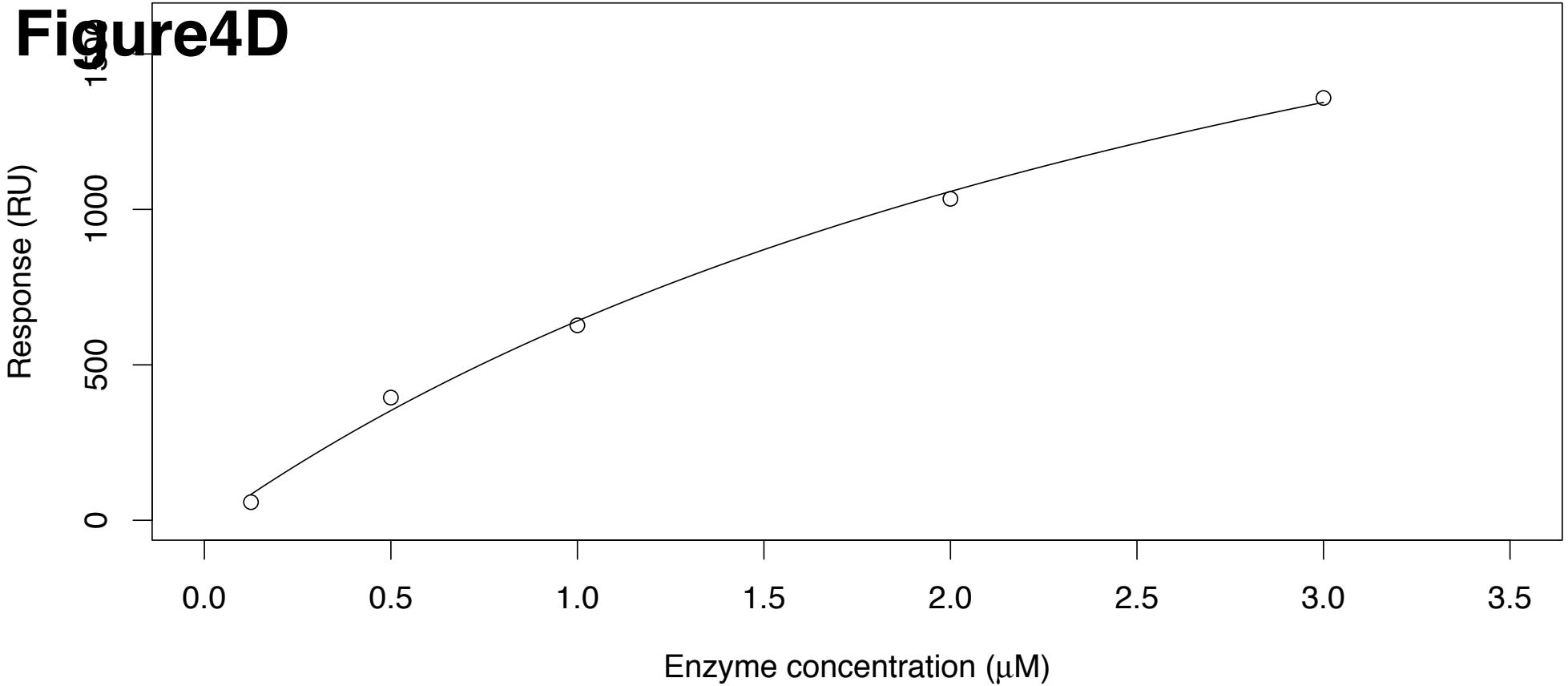
Response (RU)
0
500
1000
0.0
0.5
1.0
1.5
2.0
2.5
3.0
3.5
Enzyme concentration (μM)

Two homologous neutrophil serine proteases bind to POPC vesicles with different affinities: when aromatic amino acids matter

Anne-Sophie SCHILLINGER[1,2], Cédric GRAUFFEL[1,2], Øyvind HALSKAU[1], Nathalie REUTER[1,2*]

SUPPORTING INFORMATION

Figure S1
RMSD along the MD trajectory calculated for PR3 (grey) and HNE (green), with respect to the enzyme structure used as starting point for the simulation (enzyme structure solvated and minimized).

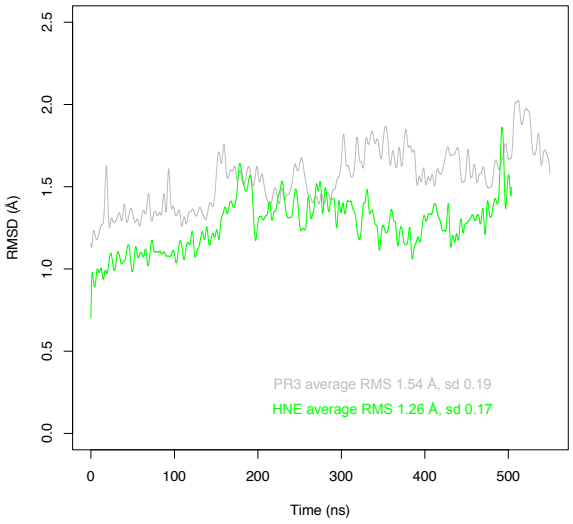

Figure S2
Distance of the center of mass of PR3 (grey) and HNE (green) to the average plane of the phosphorus atoms. Negative values indicate that the center of mass lies in the water slab above the phosphorus atoms.

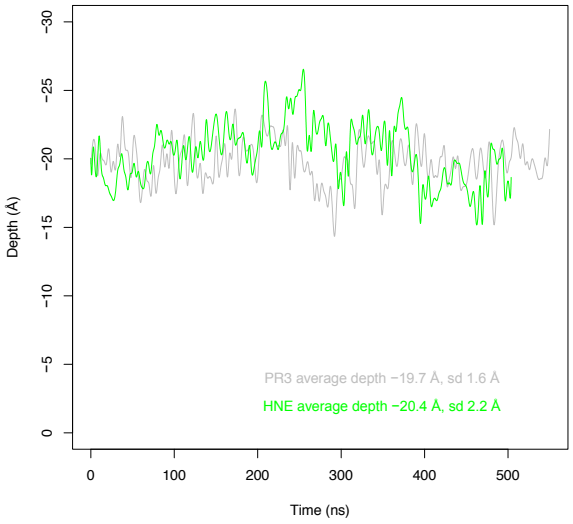

Figure S3
Depth of anchorage along simulation time calculated for amino acids Arg 146 (loop β7-β8), Arg177 (loop β8-β9), Arg178 (loop β8-β9) and Arg186 (loop β9-β10). The depth is calculated as described in the Methods section, positive values indicate that the center of mass of the amino acid is buried in the bilayer beyond the plane defined by the phosphate groups.